Residual Stress in HVOF Thermally Sprayed WC-10Co-4Cr Coating in Landing Gear Application

M. Gui[1] · R. Eybel[1] · S. Radhakrishnan[1] · F. Monerie-Moulin[2] · R. Raininger[1] · P. Taylor[2]

Abstract Type "N" Almen strips were HVOF thermally sprayed WC-10%Co-4Cr coating with spraying parameters used for landing gear coating production. The Almen strips were coated at variable passes and different cooling conditions. Deflections of Almen strip specimens were measured, and the coating residual stresses were calculated. With the same facility and spraying parameters, in situ coating property sensor was also used to continuously monitor the curvature of beam specimens being coated during and after coating deposition to evaluate coating deposition stress and final residual stress. The experiments, together with micro-hardness test, reveal that peening action occurred in the current HVOF spraying is limited, and the residual stress in the coating is dominated by quenching stress and cooling stress. In this study, the substrate temperature of specimens was adjusted by cooling air flow and torch recess time in between spraying passes. The coating residual stress demonstrates to apparently relate the substrate temperature because it significantly affects the cooling stress. Since the spraying parameters are frozen in industrial coating production, the cooling condition is a feasible approach for tailoring the coating residual stress.

Keywords Almen strip · cooling condition · HVOF thermal spraying · residual stress · WC-Co coating

✉ M. Gui
max.gui@safrangroup.com

1   Safran Landing Systems Canada Inc., Toronto, ON, Canada

2   Safran Landing Systems Bidos, Oloron Sainte-Marie Cedex, France

Introduction

HVOF-sprayed WC-Co coatings show superior wear resistance and adequate corrosion resistance. As an alternative to electroplating hard chrome, the coatings have been increasingly used in aircraft landing gears (Ref 1-4).

The residual stress in the HVOF-sprayed WC-Co coatings is found affecting the mechanical behavior and durability of the coatings, e.g., fatigue resistance and coating spallation. In accordance with SAE Aerospace Material Specification AMS2448, the residual stress shall be compressive and is evaluated by the deflection of type "N" Almen strip as 0.075 to 0.30 mm, i.e., 146 to 586 MPa calculated by Stoney equation, when it is sprayed to 0.127 mm thick coating. Aircraft landing gears work in reciprocal stress circumstance, so the fatigue performance of the material used for making landing gear parts is significant. HVOF spraying process can induce a compressive residual stress in the WC-Co coatings (Ref 5-9). However, the Cr plating process generates a high tensile residual stress and micro-cracks in the coating (Ref 10). Compressive residual stress tends to retard the nucleation and propagation of crack in the coatings in fatigue condition. So high-strength steel specimens with WC-Co coatings deposited by HVOF process demonstrate better fatigue strength compared with hard Cr plating (Ref 11-13).

In HVOF spraying process, there are three types of stress, i.e., quenching stress, peening stress and cooling stress generated during and after coating deposition. When molten or semi-molten droplets impinge on a substrate or previous coating layer, the droplets quickly solidify into thin coating splats and cool down to substrate temperature. In this circumstance, thermal contraction of the splats is constrained by underlying solid material, resulting in a tensile stress within the splats, referred to as quenching

stress. After deposition session, the coated component will cool down to ambient temperature; the mismatch in thermal expansion between the coating and the substrate will cause a cooling stress in the coating. In addition, feedstock droplets in HVOF flame impinge onto substrate or pre-deposited coating layer at a high velocity. The impingement can cause plastic deformation on the surface of underlying material and result in a compressive peening stress. In HVOF-sprayed 316L stainless steel coating, it has been reported that the peening stress is very significant (Ref 14). Generally, final residual stress in a coating produced in HVOF spraying is determined by a combination of quenching, peening and cooling stresses.

Residual stresses in HVOF thermally sprayed WC-Co coatings have been extensively studied by x-ray diffraction test and other experimental methods (Ref 7, 9, 11, 13-15), as well as finite-element (FE) simulation technique (Ref 16-18). Curvature measurement of a coating specimen is another common method used to evaluate residual stress in HVOF thermal spraying (Ref 5, 8, 15). Particularly, this method has been developed to in situ monitor coating stress development during and after the coating deposition session (Ref 14, 19-22). Almen strip is a type of specimen with dimensions and compositions specified in SAE J442. It is initially developed for shot peening process to evaluate residual stress induced in the strip by measuring its curvature, i.e., deflection, after shot peening. Almen strip has been further introduced in HVOF thermal spraying process for evaluating coating residual stress, as required in AMS 2448. After coating application, Almen strip might be bended and the deflection of the specimen can demonstrate the type and the level of residual stress in the coating.

In this study, type "N" Almen strips are HVOF thermally sprayed WC-10Co-4Cr coating at the same spraying parameters used for industrial coating production. The strips are sprayed at variable passes and different cooling conditions. Deflections of coated Almen strips are measured, and based on the measurements the coating residual stresses are calculated by Stoney equation. Also, the coating stress during and after coating deposition session is evaluated by in situ coating property (ICP) sensor. The objective of the present study is to reveal how quenching, peening and cooling stresses make contribution to the residual stress in the HVOF thermally sprayed coating. Therefore, a suitable means would be found to control the coating residual stress in landing gear industrial coating application.

Experimental Methods

Specimen and Powder Feedstock

Standard type "N" Almen strip with the size of $76 \times 19 \times 0.8$ mm, produced in Electronics Inc., is SAE 1070 cold-rolled steel with hardness of 44-50 HRC.

Feedstock used in the present study is Kennametal Stellite JK120H powder, agglomerated and sintered 86 wt.% WC-10 wt.% Co-4 wt.% Cr powder. Composition and size of the powder are shown in Tables 1 and 2, respectively. Morphology of the feedstock powder is shown in Fig. 1 obtained by SU3500 scanning electron microscope (SEM). Most powder particles are sphere-like shape.

HVOF Thermal Spray Facility

Stellite Coatings Jet Kote III HVOF system was used for coating spray. HVOF torch, JK3000, was manipulated by a FANUC M-710iB robot. One horizontal lathe is used to hold and rotate a part or specimen fixture in the process. Part rotation speed, and torch transverse speed, and torch recess time in between two consecutive spraying passes were set up in robot program.

HVOF Spraying Process

Hydrogen and nitrogen were used as fuel gas and carrier gas, respectively. The same HVOF spraying parameters listed in Table 3 were used in all the spraying experiments.

Prior to the spraying, Almen strips were cleaned by acetone and grit-blasted on both sides at 25 psi with 60 mesh Al_2O_3 grit, to minimize the curvature of the strips less than 0.05 mm arc height. The Almen strips after grit blasting measured arc height by digital Almen gauge specified in SAE J442, then firmly clamped on machined flat areas on a Φ 178 mm circular drum fixture by four screws located as indicated in SAE J442, with the convex side in the up position. Any bending behavior of the strips is fully restrained during the spraying process until the four screws are loosened. This test only discloses the final overall residual stress. When spraying, the drum fixture with Almen strips is rotated by HVOF lathe and the HVOF gun travels linearly along the axis of the fixture at 152 mm

Table 1 Chemical composition of WC-10Co-4Cr powder used for HVOF spraying

Element	wt.%
C	5.4
Co	9.9
Cr	3.6
W	81.1

Table 2 Particle size distribution of WC-10Co-4Cr powder used for HVOF spraying

Particle size, μm	vol.%
< 11	6.2
11-22	42.8
22-44	43.8
44-62	7.0
> 62	0.2

concave side, the curvature has negative sign and the coating is in tension.

The coating residual stresses in Almen strip specimens are calculated by modified Stoney formula as follows (Ref 18, 23):

Fig. 1 SEM micrographs showing morphology of WC-10Co-4Cr powder (a) at low magnification and (b) at high magnification

$$\sigma_r = \frac{[E_s t_s^2]\kappa}{6(1 - v_s)t_c} \tag{Eq 1}$$

where E_s, t_s, v_s, t_c and κ are Young's modulus of the coating specimen substrate such as Almen strip, the substrate thickness, the substrate Poisson's ratio, the coating thickness and the curvature of coating specimen derived from deflection, respectively.
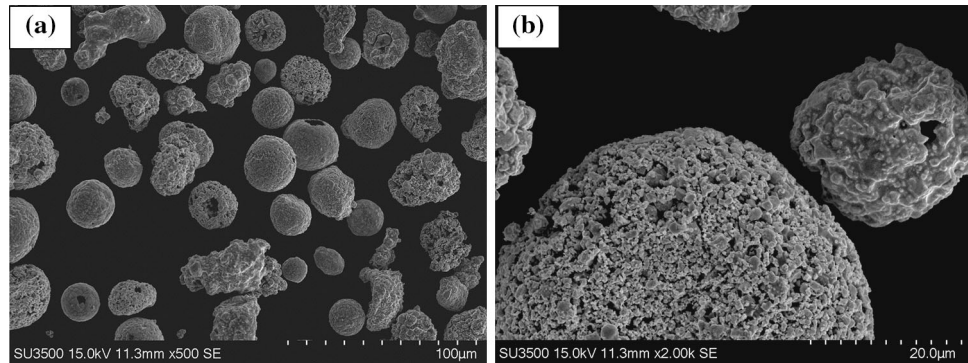
Table 3 HVOF-sprayed parameters

Items	Values
Oxygen flow, SCFH	610
Hydrogen flow, SCFH	1450
Nitrogen flow, SCFH	57
Powder feed rate, g/min	32
Spray distance, mm	152

During the spraying, the specimen fixture was cooled by compressed air at a certain pressure. A manual valve was used to adjust the air flow for the cooling. The Almen strips were HVOF-sprayed at two different surface speeds of 45.7 m/min (150 ft/min) and 91.4 m/min (300 ft/min), which are converted to rotation speeds of the fixture as 82 and 164 rpm. HVOF torch transverse speed was 4.4 mm/s at 82 rpm and 7 mm/s at 164 rpm. These two test conditions would give different coating deposition rate, i.e., coating thickness per pass. Almen strips were sprayed for 1 single pass, 2, 5 and 15 passes at 82 rpm and 1 single pass, 2, 9 and 25 passes at 164 rpm. Coating thickness on the specimens was measured by a calibrated micrometer with flat anvils. In order to achieve different substrate temperature in the spraying process at each rotation speed, the cooling condition of substrate was varied by changing cooling air flow and torch recess time in between spraying passes.

An Accuraspray G3 sensor, product of Tecnar, was used to measure and record temperature and velocity of in-flight particles in HVOF flame at the same standoff distance of 152 mm used for spraying specimens in this study. The device acquires data at each second.

standoff distance to the surface of the strips. The more details can be found in the literature (Ref 2). No preheat cycle was used to preheat specimens prior to coating application. All coating application runs started with the drum fixture at room temperature. The substrate temperature during the spraying was measured by a Raytek infrared (IR) thermometer with setting it adjacent to Almen strips being sprayed. Three Almen strips were coated in each spraying run. Coated Almen strips were removed from the drum fixture after cooling down to room temperature and measured arc height. The net deflections of Almen strips, i.e., the arc height differences between coated and grit-blasted Almen strips, are used to evaluate the coating residual stress. When measuring the arc height, un-coated surface of Almen strip was placed on four posts of the Almen gauge. By following AMS 2448, curvature sign convention for Almen strip test is described as: if Almen strip is bending with the coating in the convex side, the curvature has positive sign and the coating is in compression; if Almen strip is bending with the coating in the

With ICP sensor, product of Reliacoat Technologies, 230 × 25.4 × 2.3 mm low-carbon steel beam specimen was sprayed with the same HVOF facility and spraying parameters used for spraying Almen strips. The beam specimen is mounted on a standing fixture with free for bending. The ICP sensor can continuously monitor the stress-induced curvature by a laser sensor and measure substrate temperature by thermocouples in contact to the back of the specimen during and after coating deposition session. This method can reveal deposition stress occurred during coating deposition session, and cooling stress generated in cooling session after coating deposition; so ICP measurement can isolate deposition stress and cooling stress contribution to the final residual stress. The details of the measurement procedure are reported in Ref 19. In ICP test, specimen stands static, and HVOF torch moves in raster at 36 m/min speed and with 3 mm step distance between strokes. Two types of experiment were carried out in ICP test, one without cooling air setup and another with cooling air setup. Coating application continued without torch recess until the whole spraying cycle completed. 25 passes were sprayed on the specimen in each test. Curvature sign convention for ICP test is as follows: when beam specimen is bending with the coating in the concave side, the curvature is positive (the coating is in tension); otherwise is negative sign (Ref 21). It is remarked that the curvature sign convention in ICP test is opposite way used in Almen strip test. By Stoney formula Eq 1, the coating stresses can be calculated based on the in situ measured curvature to disclose coating deposition stress and residual stress.

Specimen Evaluation

Coated Almen strips were cross sectioned by low-speed diamond blade with coating in compression. The cutoff sections were hot-mounted by epoxy resin. The mounted specimens was roughly removed minimum 0.38 mm before final auto-grinding and polishing to avoid the effect of sectioning process on coating quality. Coating microstructure and porosity quantitative analysis were evaluated by Leica DMILM optical microscope equipped with Clemex image analysis system at 400 magnifications. The coating microstructure was also evaluated by scanning electron microscope (SEM) SU3500. Micro-hardness test of coating and Almen strip substrate was carried out with LECO M-400-G Hardness Tester at a load force of 100 grams for coating and 50 grams for metal substrate material.

Results

Particle Velocity and Temperature in the Flame

Particle temperature and velocity in HVOF flame were measured and recorded prior to and after coating deposition session by Accuraspray G3. The measuring was taken for 1-2 min at each measurement. Figure 2 illustrates the typical temperature and velocity charts of in-flight particles in the flame. The average particle temperature and velocity in HVOF flame are about 1950 °C and 645 m/s.

Coating Thickness, Substrate Temperature and Deflection in Almen Strip Test

In all the experiments performed in this paragraph, the spraying conditions are kept the same, including cooling air pressure and flow, cooling tool setup, pre-start substrate temperature and torch recess time (there is no recess time).

Figure 3 shows the coating thickness, measured by micrometer with flat anvils, on Almen strips with variable spraying pass. For both rotation speeds of 82 rpm and 164 rpm, linear relationships are clearly exhibited between coating thickness and spraying pass. It demonstrates that the thermal spraying system runs quite consistently, and the deposition rate is well controlled. Except 1 and 2 spray passes used for both of 82 and 164 rpm, at the other test points Almen strips are run with different spray passes. The purpose is to obtain equal coating thickness on the specimens at the two rotation speeds. As shown in Fig. 3, the coating thicknesses at 82 rpm with 5 and 15 passes are identical to those at 164 rpm with 9 and 25 passes. It has been known that the deflection of coated Almen strip is related to coating thickness (Ref 7). So the equal coating
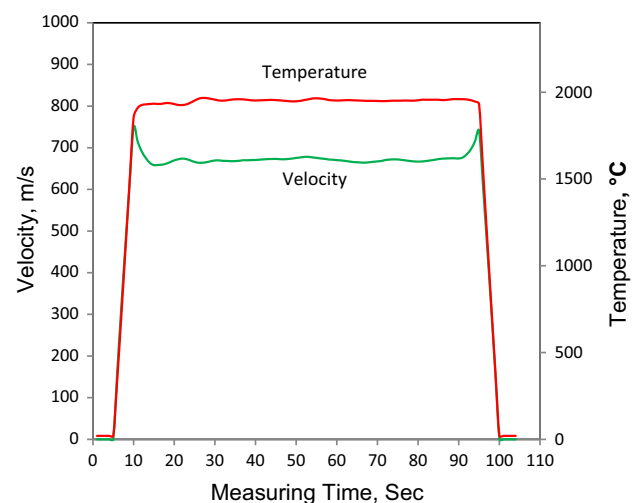

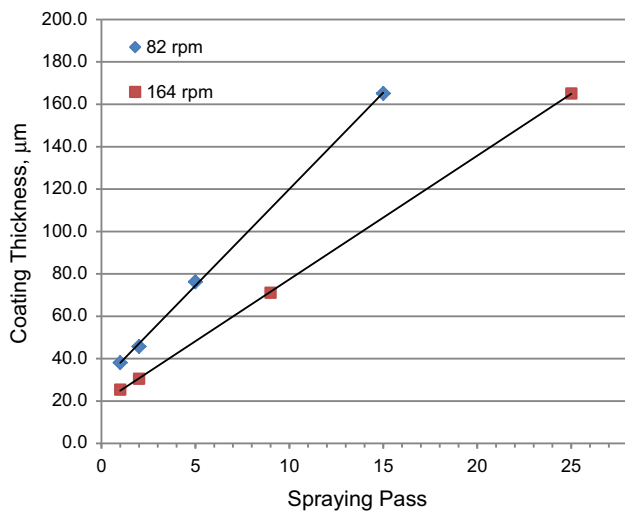**Fig. 2** Temperature and velocity charts of in-flight particles in HVOF flame measured by Accuraspray G3 sensor

Fig. 3 Coating thickness on Almen strip specimens with variable spraying passes at two rotation speeds
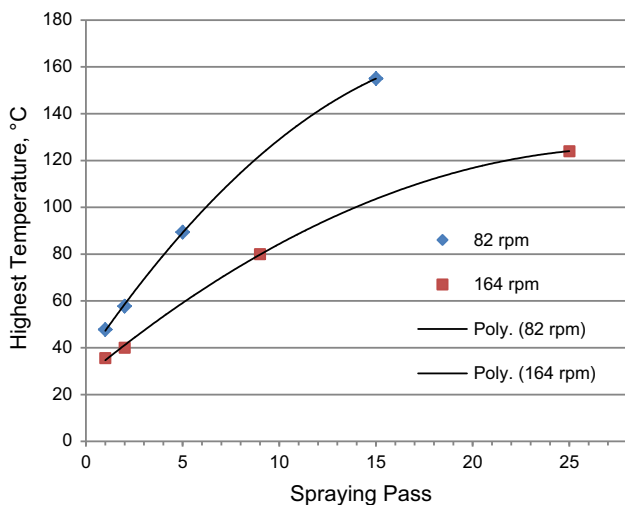

Fig. 4 Highest substrate temperature with variable spraying passes at two rotation speeds for Almen strip specimens. The curves are data's polynomial trend lines

thickness would eliminate the effect of coating thickness on Almen strip deflection. At the lower rotation speed of 82 rpm, more coating at each pass deposits onto the specimen than at the higher speed of 164 rpm since HVOF torch traverses slowly in the spraying at 82 rpm. The deposition rates are 8.7 μm/pass at 82 rpm and 5.5 μm/pass at 164 rpm.

Figure 4 shows the highest substrate temperatures in the HVOF spraying at each run. The highest temperature always concurs at last spraying pass. The highest temperatures at the lower rotation speed of 82 rpm are observed greater than those at the higher speed 164 rpm. It is because more coating deposit at each pass carries more

heat transferred into the substrate, and also because it has a longer spraying time in each pass due to a low torch speed.

Individual and average deflections of Almen strip coating specimens sprayed with different passes are shown in Fig. 5(a). The deflections of Almen strip specimens at all tests are positive value, so the residual stresses created in the coating are all compressive stress (negative value). The deflections of Almen strips sprayed in one single pass are very small, with the average of 0.0224 mm at 82 rpm and 0.0093 mm at 164 rpm. The increase in spraying pass increases the specimen deflection at the both of 164 rpm and 82 rpm. Based on the deflections, residual stresses of the coating are calculated by Stoney formula Eq 1. In the calculation, Young's modulus of 205 GPa and Poisson's ratio of 0.29 were used for Almen strip SAE 1070 steel. Calculated individual and average coating residual stresses of Almen strip coating specimens at different spraying passes are shown in Fig. 5(b). It is found that, not behaving like the deflection, the coating residual stress does not always increase as increasing spraying pass. The coating residual stress is related to the coating thickness, the deflection (curvature) of specimen and the substrate temperature.

Table 4 summarizes test results of Almen strip coating specimens in variable spraying pass practice, including coating thickness, highest substrate temperature, average deflection, average coating stress calculated by Eq 1.

In Situ ICP Test

Figure 6(a) shows the curvatures of beam specimens with spraying time measured by ICP sensor during and after coating deposition at two cooling conditions. In the figure, the period from point A to B indicates coating deposition session (the feedstock droplets are being deposited onto the specimen), and the period from point B to C indicates cooling session after coating deposition. During the coating deposition, the positive curvatures are increasing with spraying passes at both test conditions. The deposition stresses formed in the coating at both conditions are tensile stress. After the deposition, the coated specimens cool down to ambient temperature. A cooling stress will be created in the coating because of different thermal expansions between WC coating and steel substrate. In Fig. 6(a), it is found that the curvatures are going down in the cooling session. It means that the cooling stress generated in the coating is compressive. The value and sign of final residual stress in the coating depend on the combination of tensile deposition stress and compressive cooling stress. In ICP test, the substrate temperature of beam specimen was about 300 °C without air cooling and about 120 °C with air cooling, as shown in Fig. 6(b). Calculated deposition stress and residual stress in the two conditions are shown in
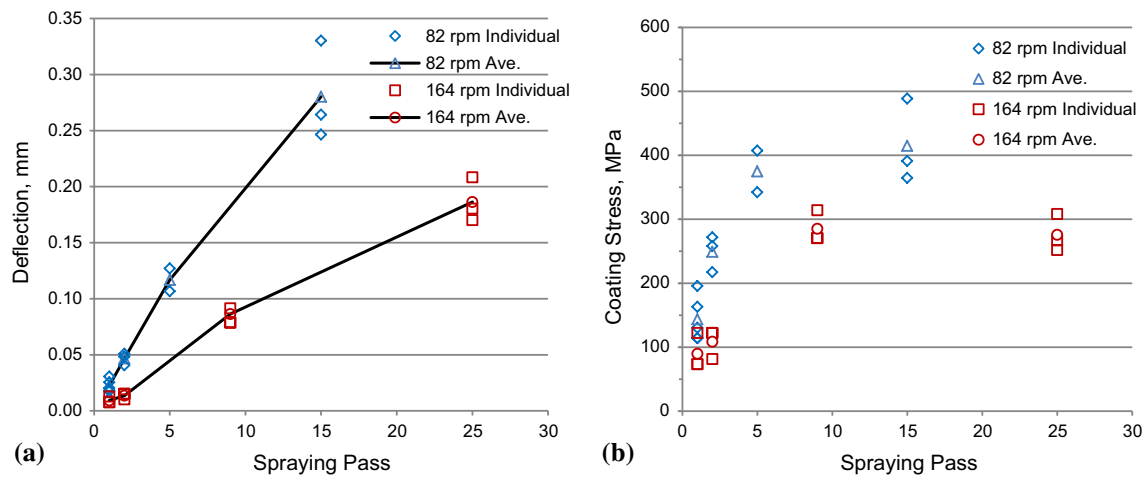
Fig. 5 (a) Individual and average deflections of coated Almen strips, (b) calculated individual and average coating stress with variable spraying passes at two rotation speeds

Table 4 Test results of Almen strip specimens in variable spraying pass practice

Rotation speed, rpm	Spraying pass	Coating thickness, μm	Highest substrate, Temp. °C	Deflection, mm	Residual stress, MPa
82	1	38.1	48	0.0224	− 143.4
	2	45.7	58	0.0466	− 248.9
	5	76.2	89	0.1168	− 374.7
	15	165.1	155	0.2808	− 414.7
164	1	25.4	36	0.0093	− 89.6
	2	30.4	40	0.0135	− 108.6
	9	71.1	80	0.0864	− 285.1
	25	165.1	124	0.1863	− 275.7

Fig. 6(c). In the condition of without air cooling, there are tensile deposition stress + 362 MPa and compressive residual stress − 194 MPa. In the condition of with air cooling, the deposition stress and residual stress are + 270 MPa and + 31 MPa, respectively; both of them are tensile stress. As a result, higher substrate temperature helps the coating approach a compressive residual stress because of more compressive cooling stress induced.

Effect of Spraying Conditions on Deflection and Residual Stress of Almen Strips Specimen

With the frozen HVOF spraying parameters, Almen strips were sprayed at different spraying conditions, i.e., different cooling air flows and torch recess times at both rotation speeds. Total spraying passes are 15 for 82 rpm and 25 for 164 rpm. Coating thicknesses in all these tests are found the very close at 165 μm. So air cooling condition and torch recess time have no effect on coating deposition rate. During the spraying, the substrate temperatures with high and low points measured by IR sensor in each spraying

pass were recorded. Figure 7 shows the substrate temperature in the spraying, the deflection of Almen strip specimens and the calculated coating residual compressive stress (average and range) in 82 rpm at three spraying conditions. Figure 8 shows the same results in 164 rpm at two spraying conditions. Not like ICP tests in Fig. 6(b), the substrate temperature in Almen strip spraying test increases gradually because the Almen strips are mounted on a big and thick drum fixture. Obviously, the deflection of Almen strip specimen depends on cooling conditions, i.e., substrate temperature. A higher substrate temperature results in a greater deflection of Almen strip coating specimen. At an identical coating thickness, the coating residual stress is directly proportional to the deflection of Almen strip specimen. The more deflection the specimen is, the more residual stress the coating has. Therefore, substrate temperature in the spraying strongly affects the coating residual stress.
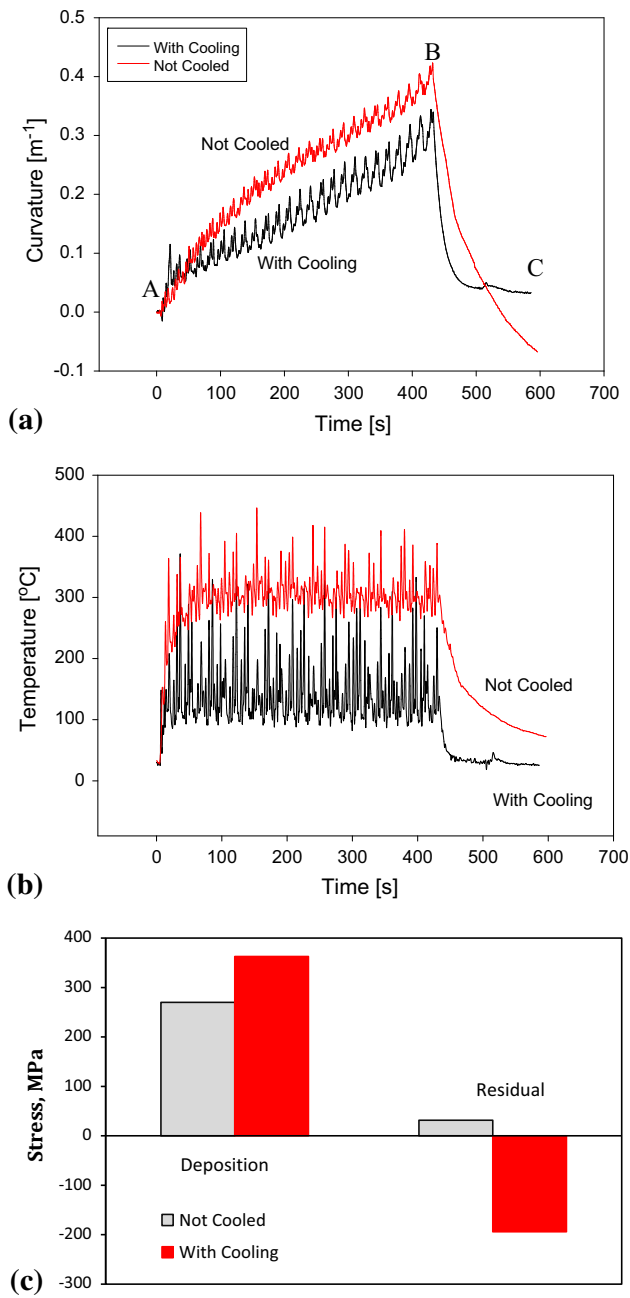
Fig. 6 (a) Curvatures of beam specimens, (b) substrate temperatures measured by ICP sensor during and after the deposition, and (c) deposition stress and residual stress

Coating Microstructure and Hardness

Figure 9 shows coating microstructures under optical microscope and SEM sprayed at 82 rpm. The coatings sprayed at all conditions have very similar microstructure. WC particulates are uniformly distributed in the coating matrix. In the coating there is no un-melted powder particle observed. Also there are no cracks and delamination seen in the coating. The coating is well bonded onto Almen strip
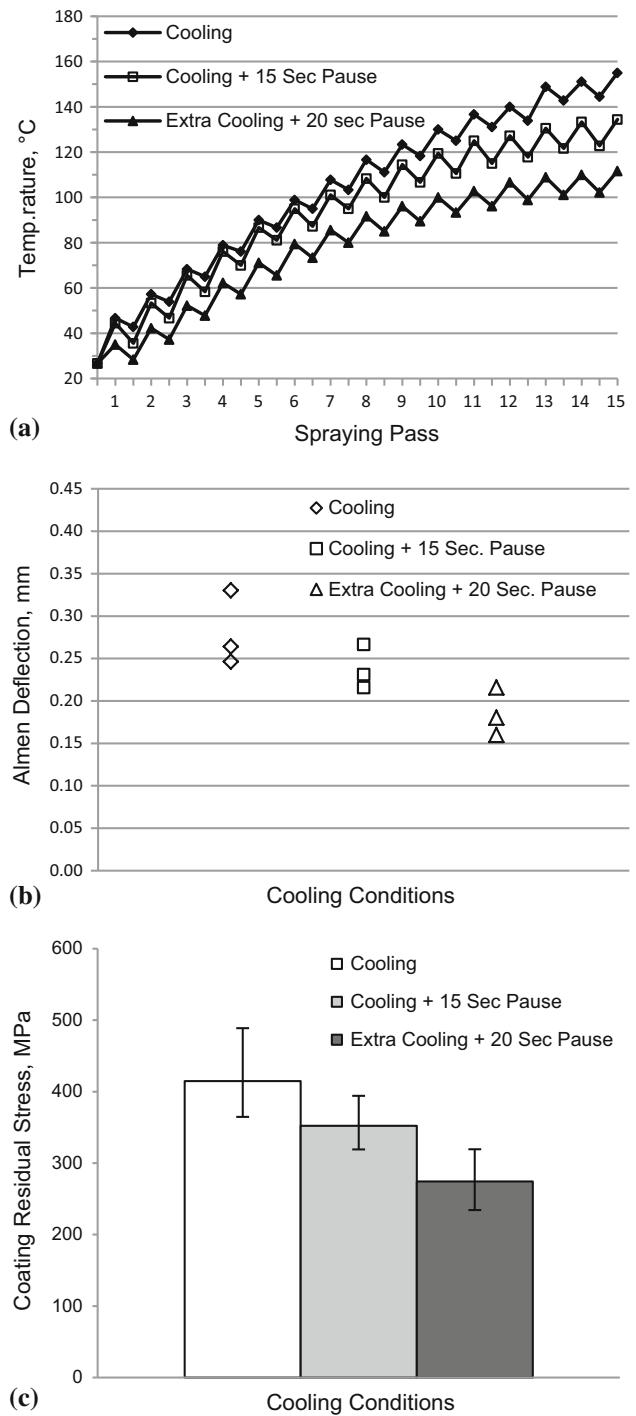

Fig. 7 Influences of cooling conditions on Almen strip specimens at 82 rpm. (a) Substrate temperature during the spraying, (b) deflections of Almen strip specimens and (c) calculated coating residual stress (average and range). "Cooling" means regular cooling air setup; "cooling + 15-s pause" regular cooling air setup plus 15-s torch recess in between passes; "extra cooling + 20-s pause" flow-enhanced cooling air setup plus 20-s torch recess in between passes

metal substrate. Table 5 shows porosity and average micro-hardness of the coatings with 165 μm thickness sprayed at
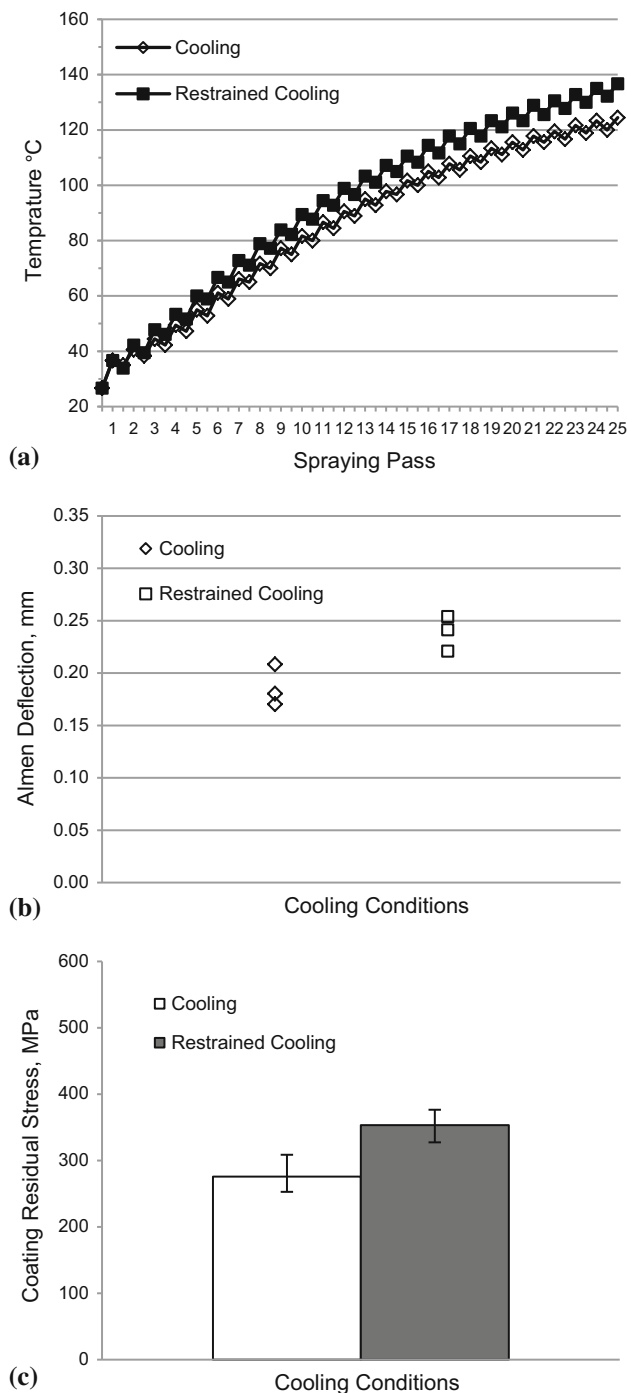
Fig. 8 Influences of cooling conditions on Almen strip coating specimen at 164 rpm. (a) Substrate temperature during the spraying, (b) deflections of Almen strip specimens and (c) calculated coating residual stress (average and range). "Cooling" means regular cooling air setup; "restrained cooling" flow-reduced cooling air setup

different spraying conditions. It reveals that cooling condition and torch recess time in between passes have no influence on the coating microstructure and hardness. As required by AMS 2448, for the coating production, the

porosity and hardness of the coating shall be $\leq 1\%$ and ≥ 950 HV, respectively.

Discussion

In general, final residual stresses in HVOF-sprayed coatings arise from three sources: quenching stress (σ_q), peening stress (σ_p) and cooling stress (σ_c). The combination of the three stresses determines the type and level of the residual stress (σ_r) in the coatings.

The quenching stress in the splats can be estimated by the equation (Ref [15]):

$$\sigma_q \approx \alpha_c \left(T_m - T_s \right) E_c \qquad (Eq\ 2)$$

where σ_q is quenching stress, α_c thermal expansion coefficient of the coating, T_m melting temperature of the coating, T_s substrate temperature and E_c elastic modulus of the coating. In this study, the coating properties, such as microstructure and hardness as indicated in Table 4, are identical in all the tests, so α_c and E_c shall be consistent in all conditions. Therefore, substrate temperature is a main factor to affect the quenching stress. A lower substrate temperature tends a higher quenching stress. WC-10Co-4Cr feedstock used in the present study is a composite powder with WC particulates mixed with matrix metals of Co and Cr. WC particulates with 2870 °C melting temperature will not be melted in HVOF flame. Melting temperature of main metal material Co in the feedstock is 1495 °C. In Eq 2, T_m in the ($T_m - T_s$) shall be identical in the present experiments because the same spraying parameters and feedstock material are used. So the ($T_m - T_s$) value mainly depends on the substrate temperature T_s. In this study, the T_s is variable, but in all cases still much lower than T_m. Therefore, the effect of the change of substrate temperature in the tests on quenching stress shall not be very significant. Additionally, when spraying Almen strip specimens, the substrate temperature T_s gradually increased with spraying pass, as shown in Fig. 7(a) and 8(a), so the quenching stress generated in splats in each pass is not the exactly equal.

ICP measurements indicate that the deposition stress in the present HVOF-sprayed WC-10Co-4Cr coating occurred during coating deposition session is tensile stress. The deposition stress σ_d originates from the balance of quenching stress σ_q and peening stress σ_p, i.e., $\sigma_d = \sigma_q$(tensile stress) $+ \sigma_p$ (compressive stress). Therefore, in the present HVOF spraying process, tensile quenching stress dominates the deposition stress. The same results in ICP test have been reported for WC-10Co-4Cr coatings by using different thermal spray facilities in other studies (Ref 24-26).

Fig. 9 HVOF WC-10Co-4Cr coating optical and SEM microstructures sprayed at 82 rpm. 15 Passes with cooling plus 15-s pause: (a) optical microscope and (b) back-scattered SEM (b); (c) 15 passes with cooling plus 20-s pause; (d) 1 single pass with cooling; (e) 2 passes with cooling; (f) 5 passes with cooling
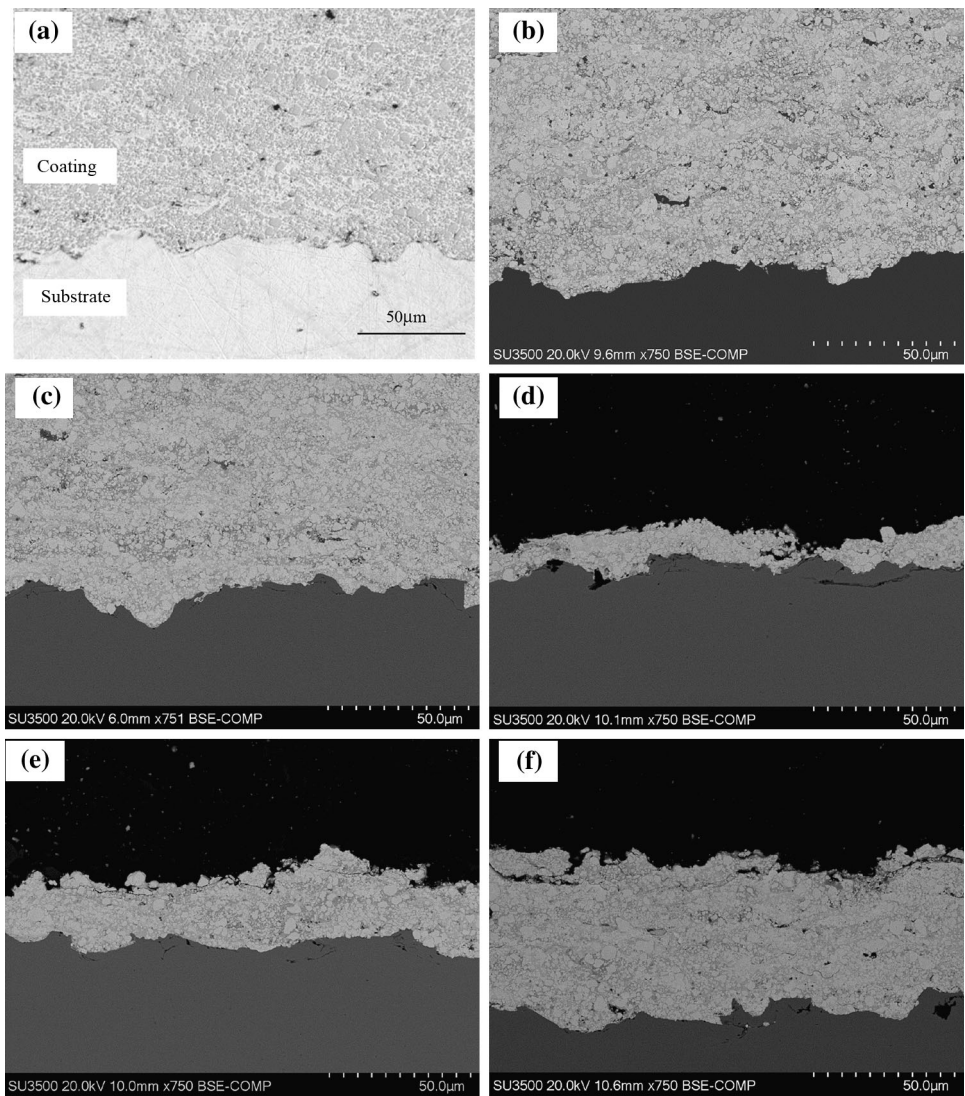

Table 5 Porosity and micro-hardness of the coatings at different spraying conditions

Spraying conditions	Porosity, %	Micro-hardness, HV$_{100gf}$
82 rpm, cooling	0.51	1233
82 rpm, cooling + 15-s pause	0.28	1271
82 rpm, extra cooling + 20-s pause	0.48	1238
164 rpm, cooling	0.31	1234
164 rpm, restrained cooling	0.32	1258

In HVOF thermal spray, kinetic energy of sprayed particles with high velocity might cause a significant compressive peening stress by plastically deforming the surface layer of target. With in situ curvature method, it has been found that the deposition stress is dominated by peening stress during the coating deposition session in HVOF-sprayed NiCr coating (Ref 21) and 316L stainless steel coating (Ref 14). Even for the same WC-CoCr coating used in the this study, the deposition stress can be also dominated by peening stress depending on the HVOF facility and spraying parameters used (Ref 22, 24, 25). In these circumstances, the deposition stresses are shown as compressive stress because the compressive peening stress overwhelms the tensile quenching stress. Generally, the higher the velocity of particles in HVOF flame is, the more kinetic energy the particles carry, therefore inducing more peening stress in deposition session (Ref 14, 21, 22). JP thermal spray system with liquid fuel produces high particle velocity at more than 800 m/s, which favors to achieve a big compressive deposition stress because of

strong peening action (Ref 22, 24). DJ thermal spray system with H$_2$ fuel gas can also generate compressive deposition stress, i.e., dominance of peening effect in deposition session, when particle velocity is higher than 700 m/s (Ref 24). In this study, particle speed in HVOF flame was measured at about 645 m/s.

In the literature (Ref 14), in situ curvatures show an abrupt stepwise change at the onset of spraying, which is caused by peening action on the substrate at the first spraying pass. Furthermore, the work hardening caused by peening action tends to increase the coating hardness when peening effect dominates deposition stress (Ref 21). In addition, the peening action can cause a variation of hardness in the 316 L stainless steel substrate and 316L coating: for the substrate, there is a layer of increased hardness on the substrate surface region at the coating/substrate interface because the substrate surface is hardened by peening action of HVOF particles; for the coating, the hardness on the coating top surface region is lower than the inside because it is not peened by the following particles (Ref 14).

In this study, tensile deposition stress during deposition session was found in ICP test; there were no abrupt stepwise drop changes seen at the first pass on the curvatures in Fig. 6(a). In Almen strip test, the single-pass spraying only caused very small increase in the deflection of specimen: net deflection 0.0224 mm at 82 rpm and 0.0093 mm at 164 rpm. A comparable test was performed on the same type "N" Almen strips by grit blasting which was used for preparing Almen strip surface before HVOF spraying. Almen strips were grit-blasted single pass on one side at 25 psi air pressure. Actually, grit blasting causes compressive peening stress on the strips by impingement of grit media. It was found that the grit blasting attained a lot higher deflection, 0.2464 mm, on the Almen strips than the HVOF single-pass spraying. Based on these studies, in the present HVOF process, the first spraying pass does not show a notable peening action on the substrate induced by impingement of feedstock droplets.

In WC-10Co-4Cr powder, main metal matrix material Co has a melting temperature T_m at 1495 °C. The temperature of in-flight particles in the HVOF flame measured by Accuraspray G3 is found greater than this point. So the base metal materials in powder feedstock shall be melted in the flame before impinging the substrate. This can be evidenced from the coating microstructure analysis that there were no un-melted feedstock particles observed in the coating microstructure. Compressive peening stress during the coating deposition is proportional to particle kinetic energy (Ref 21). Semi-melted and un-melted particles with larger mass in HVOF thermal flame have more kinetic energy and induce more peening stress when they impinge onto target (Ref 14, 21). However, in the present spraying,

feedstock powder is melted, hence weakening the peening action. Figure 10 and 11 show the micro-hardness measurements in the coating and the substrate of Almen strip specimens sprayed at 82 and 164 rpm in this study at different cooling conditions, Each test point is the average of five individual measurements. The micro-hardness does not exhibit any typical trends either in the coating or the substrate. The micro-hardness on the surface of substrate near the interface of coating and substrate has no notable difference from the inside. The micro-hardness in the coating also displays scatter distributions. It reveals that there is no significant peening action occurred in the spraying session, which causes material work hardening. These investigations disclose that the peening effect shall be slight in the current HVOF spraying process.

In ICP test in this study as shown in Fig. 6, the tensile deposition stress at "not cooled" condition is 362 MPa, greater than 270 MPa at "with cooling" condition. The substrate temperature in the former is 300 °C, higher than 120 °C in the latter. According to Eq 2, a higher substrate temperature T_s will reduce tensile quenching stress, hence tending a lower deposition tensile stress. However, the ICP test shows greater tensile deposition stress at the higher substrate temperature. The study (Ref 26) reported that higher particle temperature in HVOF flame causes higher deposition tensile stress because of better lamella cohesion. The better lamella cohesion will help to build up more quenching stress during the deposition. In this work, the same spraying parameters are used, and the particle temperature is identical at all different cooling condition runs. So the particle temperature is not the case to effect on the deposition stress. As known, deposition stress is the balance of tensile quenching stress and compressive peening stress. At higher substrate temperature, probably peening action (even not a dominant stress) during deposition session is further weakened since the higher substrate temperature may reduce plastic deformation hardening in the coating induced by high velocity particles, which causes the higher tensile deposition stress in the ICP test.

Due to the mismatch in coefficients of thermal expansion (CTE) between coating and substrate, a cooling stress, σ_c, will be generated in the coating when cooling down to room temperature after coating deposition session. The stress can be estimated by the following equation (Ref 15):

$$\sigma_c = \frac{[E_c(T_s - T_r)(\alpha_c - \alpha_s)]}{\left[1 + 2\left(\frac{E_c t_c}{E_s t_s}\right)\right]} \qquad \text{(Eq 3)}$$

where E_s is the substrate elastic modulus, α_c, T_r, t_s and t_c are substrate CTE, room temperature, and thickness of the substrate and thickness of coating, respectively. In this study, for Almen strip specimen, substrate thickness t_s is 0.8 mm, and the greatest coating thickness t_c is 0.165 mm.

Fig. 10 Micro-hardness measurements in the coating and Almen strip substrate at different cooling conditions at 82 rpm
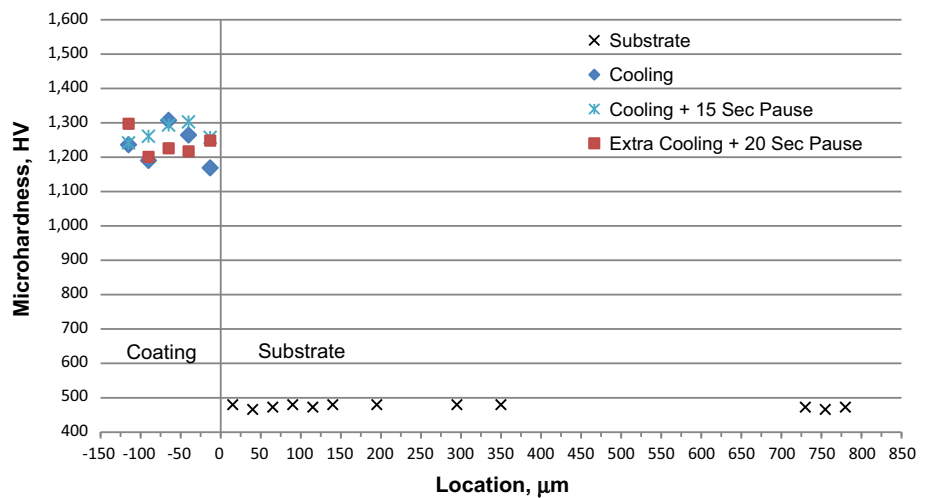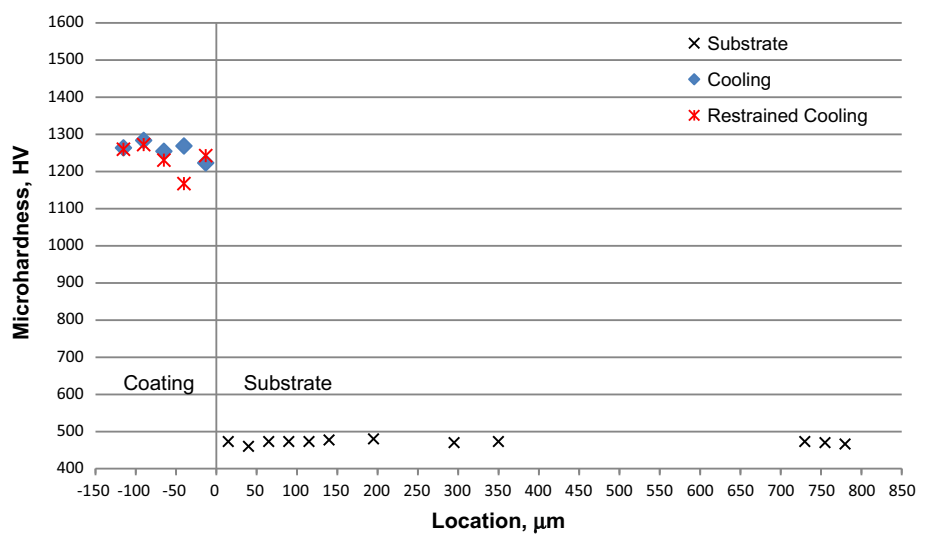

Fig. 11 Micro-hardness measurements in the coating and Almen strip substrate at different cooling conditions at 164 rpm

The cooling stress is proportional to the difference of CTEs between the coating and the substrate. For WC-10Co-4Cr powder feedstock used in this study, the most content in the coating is WC particles as shown in Fig. 9. WC has a very low CTE at about 5.5×10^{-6}/°C. The CTE of WC-10Co-4Cr coating is estimated at 6.5×10^{-6}/°C by the rule of mixtures based on the nominal chemical composition of the powder. In the Almen strip spraying test, CTE of the substrate (SAE 1070) is 11.6×10^{-6}/°C. Obviously, the coating has a much lower CTE than the substrate, and a compressive cooling stress will be generated in the coating. In Eq 3, as described before, α_c and E_c shall be constant in this study, and for a standard substrate specimen like Almen strip, E_s and t_s have no change. Therefore, at an identical coating thickness, the factor to affect the cooling stress is only the substrate temperature T_s. A higher substrate temperature shall result in a higher compressive cooling stress, which enhances the coating to have a compressive residual stress. This has been validated in both Almen strip test and ICP test.

In this study, all coatings produced in Almen strip tests with air cooling have compressive residual stress. However, the coating obtained in ICP test at cooling condition shows a tensile residual stress, even just a small value at 31 MPa. A tensile residual stress in HVOF-sprayed WC-10Co-4Cr coating has been reported in ICP test in other studies (Ref 24, 26). The sign of the coating residual stress can be tailored as positive (tensile stress), negative (compressive stress) and neutron (no stress) by varying spraying parameters and cooling conditions (Ref 25). Currently, the same spraying parameters are used, and cooling conditions, i.e., substrate temperatures, are comparable in Almen strip tests and the ICP test; but the two test methods show somehow results difference. As described before, Almen strip test restrains the bending of specimen from quenching action during coating deposition session, whereas in ICP test the specimen is freely bended from quenching action.

These can cause quenching behavior difference in the two test methods and affect the final coating residual stress.

Conclusions

The present HVOF spraying practice demonstrates that cooling condition and torch recess time have no effect on coating deposition rate and coating properties such as porosity and hardness.

The application of HVOF thermally sprayed WC-10Co-4Cr coatings in landing gears highlights residual stress in the coatings. In this study, industrial HVOF thermal spray equipment and spraying parameters are used to spray coating specimens. The stresses formed in the coating are investigated by type "N" Almen strips and in situ coating property (ICP) sensor. It is found that the peening action occurred in the current HVOF spraying is limited compared with quenching stress and cooling stress. ICP test demonstrates that deposition stress developed in the coating during coating deposition session is tensile stress, dominated by quenching stress. The overall residual stress in the WC-10Co-4Cr coating is mainly contributed by tensile quenching stress during deposition session and compressive cooling stress after deposition session.

In industrial coating production, thermal spraying parameters run as a frozen recipe and are no longer varied to remedy the coating residual stress. The part cooling condition, which influences substrate temperature, therefore cooling stress, is a feasible means to be managed to control the residual stress.

References

1. D. Lee, R. Eybel, and R. Evans, Development and Implementation of HVOF WC/Co/Cr Coating as Alternative to Electrolytic Hard Chrome Plate in Landing Gear Applications Using Natural Gas As Fuel, Thermal Spray 2003: Advancing the Science and Applying the Technology, *ASM Int.*, 2003, **2003**, p 371-376

2. M. Gui, R. Eybel, B. Asselin, and F. Mouerie-Moulin, Cracking and Spalling Behavior of HVOF Thermally Sprayed WC-Co-Cr Coating in Bend and Axial Fatigue Tests, *J. Mater. Eng. Perform.*, 2015, **24**(3), p 1347-1356

3. B. Evans, R. Panza-Giosa, E. Cochien Brikaras, and S. Maitland, HVOF-Applied WC-Co-Cr as a Hard Chrome Replacement for Landing Gear, Thermal Spray 2006: Science, Innovation, and Application: Proceedings of the Spray Conference, *ASM Int.*, 2006, **2006**, p 615-617

4. P.F. Ruggiero, Tungsten Carbide Coatings Replace Chromium, *Adv. Mater. Process.*, 2005, **163**(7), p 39-40

5. J. P. Sauer and P. Sahoo, HVOF Process Control Using Almen and Temperature Measurement, Thermal Spray 2001: New Surface for a New Millennium: Proceedings of the International Thermal Spray Conference, *ASM Int.*, 2001, 791–796

6. J.G. Legoux, S. Bouaricha, and J.P. Sauer, Cracking and Spalling Behavior of WC-17% Co Cermet Coating, Thermal Spray 2006: Science, Innovation and Application: Proceeding of the Spray Conference, *ASM Int.*, 2006, **2006**, p 609-616

7. U. Selvadurai, P. Hollingsworth, I. Baumann, B. Hussong, W. Tillmann, S. Rausch, and D. Biermann, Influence of the Handling Paramters on Residual Stresses of HVOF-Sprayed WC-12Co Coatings, *Surf. Coat. Technol.*, 2015, **268**, p 20-35

8. M. Gui, R. Eybel, B. Asselin, S. Radhakrishanan, and J. Cerps, Influence of Processing Parameters on Residual Stress of High Velocity Oxy-Fuel Thermally Sprayed WC-Co-Cr Coating, *J. Mater. Eng. Perform.*, 2010, **21**(10), p 2090-2098

9. A.K. Maiti, N. Mukhopadhyaym, and R. Rman, Improving the Wear Behavior of WC-CoCr-Based HVOF Coating by Surface Grinding, *J. Mater. Eng. Perform.*, 2009, **18**, p 1060-1066

10. W. Pfeiffer, C. Koplin, E. Reisacher, and J. Wenzel, Residual Stresses and Strength of Hard Chromium Coatings, *Mater. Sci. Forum*, 2011, **681**, p 133-138

11. H.J.C. Voorwald, R.C. Souza, W.L. Pigatin, and M.O.H. Cioffi, Evaluation of WC-17Co and WC-10Co-4Cr Thermal Spray Coatings by HVOF on the Fatigue and Corrosion Strength of AISI, 4340 Steel, *Surf. Coat. Technol.*, 2005, **190**, p 155-164

12. A. Aguero, F. Camon, J. Garcia de Blas, J.C. del Hoyo, R. Muelas, A. Santaballa, S. Ulargui, and P. Valles, HVOF-Deposited WCCoCr as Replacement for Hard Cr in Landing Gear Actuators, *J. Therm. Spray Technol.*, 2011, **20**, p 1292-1309

13. A. Ibrahim and C.C. Berndt, Fatigue and Deformation of HVOF Sprayed WC-Co Coatings and Hard Chrome Plating, *Mater. Sci. Eng. A*, 2007, **456**, p 114-119

14. S. Kuroda, Y. Tashiro, H. Yumoto, S. Taira, H. Fukanuma, and S. Tobe, Peening Action and Residual Stresses in High-Velocity Oxygen Fuel Thermal Spraying of 316L Stainless Steel, *J. Therm. Spray Technol.*, 2001, **10**, p 367-374

15. J. Stokes L. Looney, Residual Stress in HVOF Thermally Sprayed Thick Deposits, *Surf. Coat. Technol.*, 2004, **177–178**, p 18–23

16. G. Montay, A. Cherouat, A. Nussair, and J. Lu, Residual Stress in Coating Technology, *J. Mater. Sci. Technol.*, 2004, **20**, p 81-84

17. P. Bansal, P.H. Shipway, and S.B. Leen, Effect of Particle Impact on Residual Stress Development in HVOF Sprayed Coatings, *J. Therm. Spray Technol.*, 2006, **15**, p 570-575

18. J. Stokes and L. Looney, Predicting Quenching and Cooling Stresses within HVOF Deposits, *J. Therm. Spray Technol.*, 2008, **17**, p 908-914

19. J. Matejicek and S. Sampath, In-Situ Measurement of Residual Stresses and Elastic Moduli in Thermal Sprayed Coatings: Part 1: Apparatus and Analysis, *Acta Mater.*, 2003, **51**, p 863-872

20. A. Valarezo, G. Bolelli, V.B. Choi, S. Sampath, V. Canillo, L. Lusvarghi, and R. Rosa, Damage Tolerant Functionally Graded WC-Co/Stainless Steel HVOF coating, *Surf. Coat. Technol.*, 2010, **205**, p 2197-2208

21. A. Valarezo and S. Sampath, An Integrated Assessment of Process–Microstructure–Property Relationships for Thermal-Sprayed NiCr Coatings, *J. Therm. Spray Technol.*, 2011, **20**, p 1244-1258

22. A. Vackel, G. Dwived, and S. Sampath, Structurally Integrated, Damage-Tolerant, Thermal Spray Coatings, *JOM*, 2015, **67**, p 1540-1553

23. T.W. Clyne and S.C. Gill, Residual Stresses in Thermal Sprayed Coatings and Their Effect on Interfacial Adhesion: A Review of Recent Work, *J. Therm. Spray Technol.*, 1996, **5**, p 401-418

24. A. Vackel, G. Dwivedi, and S. Sampath, Influence of In-Flight Particle States on Particle Peening Intensity and Related Properties of HVOF WC-CoCr Coatings, *Therm. Spray Bull.*, 2015, **8**(1), p 32-41

25. A. Vackel and S. Sampath, Fatigue Behavior of Thermal Sprayed WC-CoCr-Steel Systems: Role of Process and Deposition Parameters, *Sur. Coat. Technol.*, 2017, **315**, p 408-416

26. T. Varis, T. Suhonenm A. Ghabchi, A. Valarezo, S. Sampath, X. Liu, and S. P. Hannula, Formation Mechanisms, Structure, and Properties of HVOF-Sprayed WC-CoCr Coatings: An Approach Toward Process Maps, *J. Therm. Spray Technol.*, 2014, **23**, p 1009–1018

Publisher's Note Springer Nature remains neutral with regard to jurisdictional claims in published maps and institutional affiliations.